Available online at www.sciencedirect.com
SCIENCE DIRECT®
PERGAMON
International Journal of Heat and Mass Transfer 46 (2003) 2947–2955
International Journal of HEAT and MASS TRANSFER
www.elsevier.com/locate/ijhmt

Confined swirling jet impingement onto an adiabatic wall

S.Z. Shuja *, B.S. Yilbas, M. Rashid

Department of Mechanical Engineering, King Fahd University of Petroleum and Minerals (KFUPM), Drahran 31261, Saudi Arabia

Received 13 February 2001; received in revised form 3 February 2003

Abstract

Impinging swirling jets generate interesting flow fields and depending on the magnitude of the swirl velocity, circulation cells develop in the region close to the solid wall. Moreover, axial momentum of the jet is influenced by the magnitude of the swirl velocity. This, in turn, results in considerable entropy generation in the flow field. In the present study, confined swirling jet impingement onto an adiabatic wall is investigated. The flow and temperature fields are computed numerically for various flow configurations. Different jet exit velocity profiles are considered and their effects on the flow field are examined. The entropy production due to different flow configurations is computed and the irreversibility ratios due to fluid friction and heat transfer are determined. It is found that the jet axis tilts towards the radial direction as swirl velocity increases and reducing the velocity profile number enhances the entropy generation due to heat transfer. The irreversibility ratio variation with the velocity profile number behaves opposite for the fluid friction and heat transfer.

Keywords: Confined swirling jet entropy analysis

1. Introduction

The flow impingements on surfaces find wide application in industry. Typical applications include tempering of glass, annealing of materials, cooling of turbine blades, drying of papers, etc. The use of a single circular jet results in a localized high heat transfer rate at the point of impingement. Introducing the swirling motion in the impinging jet enhances the flow mixing and improves the heat transfer characteristics.

Considerable research studies were carried out to explain the jet impinging process. Yang et al. [1] investigated the heat transfer due to confined impinging jet on spherically concave surfaces for piston cooling application. They indicated that as the reciprocating force modified the heat transfer from the non-reciprocating situation, this needed to account for the effect of reciprocating motion on heat transfer with-in the coolant channels of piston to achieve the optimal design of cooling systems. The hydrodynamic characteristics for a round jet impingement with annular confinement were studied by Hung and Haung [2]. They proposed a mathematical relation between the maximum stress-friction factor and the Reynolds number for parabolic and uniform flow velocity profiles. The circulation zones of unconfined and confined annular swirling jets were investigated experimentally by Sheen et al. [3]. They used the scaling analysis to calculate the length of the recirculation zone with the swirl number. The variation of heat transfer in laminar wall jets with different initial velocity profiles was studied by Korovkin and Sokovishin [4]. They investigated the effect of the shape of initial velocity profile on the development of principle hydrodynamic and thermal parameters. The near flow field of an axisymmetric water jet was investigated using a particle tracing velocimetry by Romano [5]. He showed that fluid injected in the jet centerline was observed to be converted to center-rotating vortices. The flow and heat transfer characteristics of impinging laminar jets issuing from rectangular slots of different

* Corresponding author. Tel.: +966-3-8606458; fax: +966-3-8602949.
E-mail address: shuja@ccse.kfupm.edu.sa (S.Z. Shuja).

0017-9310/03/$ - see front matter © 2003 Elsevier Science Ltd. All rights reserved.
doi:10.1016/S0017-9310(03)00073-5

Nomenclature

I	irreversibility rate (W)
ISV	inlet swirl velocity (m/s)
k	thermal conductivity (W/m K)
M	Merit number
n	velocity profile number
r	radial distance/radius (m)
r_0	jet exit diameter (m)
$\dot{S}'''_{\text{gen}}$	volumetric entropy generation rate (W/m^3 K)
T	temperature (K)
$\bar{u}_{\text{jet}}$	jet mean axial velocity (m/s)
v	velocity vector (m/s)
$V_{\max}$	maximum velocity (m/s)
v_r	velocity component in radial direction (m/s)
v_z	velocity component in axial direction (m/s)
v_θ	velocity component in tangential direction (m/s)
$\forall$	volume (m^3)
z	axial distance

Greek symbols

ϕ	arbitrary variable
μ	dynamic viscosity (N s/m^2)
ν	kinematic viscosity (m^2/s)
ρ	density (kg/m^3)
σ	Prandtl number

aspects ratios were investigated numerically by Sezai and Mohamed [6]. The effect of the off-center velocity peaks on the Nusselt number distribution was investigated and three-dimensional flow structures were detected, which could not be predicted by two-dimensional simulations. A numerical study was carried out by Lee et al. [7] to characterize the thermal behavior of laminar circular jets. They indicated that very large recovery factors, over 20, were obtained for high Prandtl number liquid jets.

The thermodynamic performance of a device, or process, can be assessed through the measure of the irreversibility generated. The second law analysis was widely used to evaluate the sources of irreversibility in flow and thermal systems. Considerable research has been carried out to examine the irreversibility generated in flow systems. The numerical predictions of local entropy generation in an impinging jet were carried out by Drost and White [8]. They indicated that calculation of local entropy generation was feasible and could provide useful information. Entropy generation due to heat transfer from discretely heated plate to an impinging confined jet was investigated by Ruocco [9]. He showed that understanding the entropy generation mechanism allowed one to assess the conjugate arrangement based on solid fluid coupling criterion. The integral analysis of two-dimensional jets and entropy generation was presented by Bejan [10]. He suggested that an important relationship existed between the empirical components of the pure fluid mechanics integral treatment and the temperature, and entropy generation extremes unveiled by the thermodynamic analysis. Entropic efficiency of energy systems was studied by Arpaci and Selamet [11]. They showed that the heat transfer from a pulse combuster became a measure for entropic efficiency of combustion systems. Second law analysis of combined heat and mass transfer in internal and external flows was carried out by Carrington and Sun [12]. They indicated that the assumption of local thermodynamic equilibrium gave wrong results due to a strong coupling term between heat and mass transfer. A study of entropy generation in fundamental convective heat transfer was carried out by Bejan [13]. He showed that flow geometric parameters might be selected in order to minimize the irreversibility associated with a specific convective heat transfer process.

In the present study, a swirling confined jet impinging onto a solid surface was considered. The effect of jet velocity profiles on the flow and thermal fields is investigated. The governing equations of flow and heat transfer are solved numerically using a control volume approach. The entropy generation due to fluid friction and heat transfer is computed. The study is extended to include the investigation of effect of swirl velocity on the flow field and entropy generation rate.

2. Mathematical analysis

The equations governing the laminar axisymmetric free jet can be written in the cylindrical coordinate system. The flow is assumed to be steady and incompressible with constant properties.

The continuity equation is

$$\nabla \cdot \mathbf{v} = 0$$

The momentum equation is

$$\rho(\mathbf{v} \cdot \nabla)\mathbf{v} = -\nabla P + \mu \nabla^2 \mathbf{v}$$

The energy equation is

$$\rho(\mathbf{v} \cdot \nabla)T = \frac{\mu}{\sigma}\nabla^2 T + \frac{\mu}{C_p}\Phi$$

where Φ is the viscous dissipation term, which is

$$\Phi = \left\{ 2\left[\left(\frac{\partial v_r}{\partial r}\right)^2 + \left(\frac{v_r}{r}\right)^2 + \left(\frac{\partial v_z}{\partial z}\right)^2 \right] + \left(\frac{\partial v_z}{\partial r} + \frac{\partial v_r}{\partial z}\right)^2 + \left(\frac{\partial v_\theta}{\partial z}\right)^2 + \left[r\frac{\partial}{\partial r}\left(\frac{v_\theta}{r}\right)\right]^2 \right\}$$

2.1. The boundary conditions

Fig. 1 shows the jet configuration and the boundary conditions. The flow velocities are set to zero along the solid walls, i.e. no slip condition is accommodated.

Inlet condition: $\bar{u}_{\text{jet}}$ = specified (0.03 m/s) and T_{jet} = specified (310 K).

Symmetric axis: The radial derivatives of the flow variables are set to zero, i.e., $\partial\phi/\partial r = 0$, where ϕ is any flow variable.

Outlet conditions: The mass continuity at the outlet of the control volume yields the corresponding boundary conditions at outlet, which are

$$\frac{\partial(r\phi)}{\partial r} = 0 \quad \text{and} \quad \frac{\partial\phi}{\partial z} = 0$$

2.2. The jet exit velocity profiles

The jet exit velocity profiles are considered as in the form of

$$v_z = V_{\max}\left(1 - \frac{r}{r_0}\right)^n$$

where $V_{\max}$ is the maximum velocity, n is the velocity profile number and r_0 is the jet radius. The values of n are 1, 1/1.5, 1/2, 1/5, 1/7, 1/10, and 1/200. The mass flow rate across the jet is kept constant, i.e. the mean velocity is constant for all jet exit velocity profiles. The Reynolds number is, therefore, kept constant at $Re = 50$ to ensure the laminar flow of free jet in the simulations.

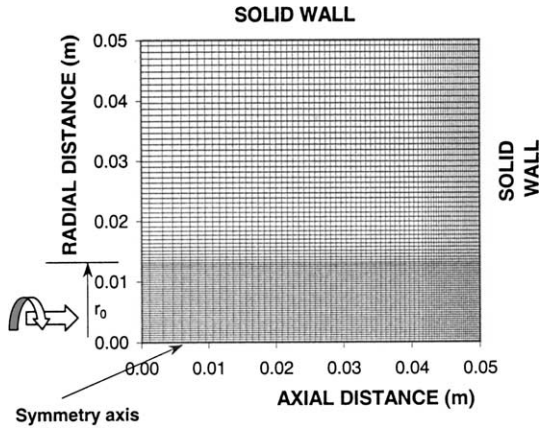

Fig. 1. Layout and grid distribution employed in the simulations. The arrows represente the jet inlet and swirl directions while r_0 (0.0127 m) is the jet radius.

3. Entropy analysis

The volumetric entropy generation rate can be formulated as [14]

$$\dot{S}'''_{\text{gen}} = \frac{k}{T^2}\left[\left(\frac{\partial T}{\partial r}\right)^2 + \left(\frac{\partial T}{\partial z}\right)^2\right] + \frac{\mu}{T}\Phi$$

The first term on the right side of the equation is the volumetric entropy generation due to the heat transfer while the second term is the contribution due to the fluid friction. The irreversibility rate associated with the flow system can be written as

$$\dot{I} = \oint_{\forall} \dot{S}'''_{\text{gen}}\, \mathrm{d}\forall$$

where $\forall$ is the volume. The irreversibility ratio, which is the ratio of irreversibility rate due to fluid friction, or heat transfer, to the total irreversibility rate due to fluid friction and heat transfer, i.e.:

$$I_{\text{Friction}} = \frac{\left(\oint_{\forall} \dot{S}'''_{\text{gen}}\, \mathrm{d}\forall\right)_{\text{Friction}}}{\left(\oint_{\forall} \dot{S}'''_{\text{gen}}\, \mathrm{d}\forall\right)_{\text{Friction}} + \left(\oint_{\forall} \dot{S}'''_{\text{gen}}\, \mathrm{d}\forall\right)_{\text{Heat Transfer}}}$$

and

$$I_{\text{Heat Transfer}} = \frac{\left(\oint_{\forall} \dot{S}'''_{\text{gen}}\, \mathrm{d}\forall\right)_{\text{Heat Transfer}}}{\left(\oint_{\forall} \dot{S}'''_{\text{gen}}\, \mathrm{d}\forall\right)_{\text{Friction}} + \left(\oint_{\forall} \dot{S}'''_{\text{gen}}\, \mathrm{d}\forall\right)_{\text{Heat Transfer}}}$$

3.1. Numerical Solution

The flow domain is overlaid with a rectangular grid (staggered grid arrangement) as shown in Fig. 1. A numerical scheme employing a control volume approach is introduced to discretize the governing equations of flow. All the variables are computed at each grid point except the velocities, which are determined midway between the grid points. The grid independent tests were conducted and a grid consisting of 80×75 grid points was selected on the basis of less computation time without compromising the grid independency. It should be noted that the convergence criteria was based on the residuals, which were set 10^{-6} during the simulations. The pressure linkages through the continuity equation, known as the SIMPLE algorithm, are used [15]. This procedure is an iterative process for convergence. The pressure link between continuity and momentum is established by transforming the continuity equation into a Poisson equation for pressure. The Poisson equation implements a pressure correction for a divergent velocity field.

4. Results and discussions

A laminar confined swirling jet impinging on an adiabatic wall is considered. The flow and temperature fields are computed numerically. Entropy generation due to fluid friction and heat transfer is obtained and the corresponding irreversibility ratios are determined. In the analysis, several jet velocity profile numbers are considered while five different swirl velocities are employed to account for the effect of swirling motion on the entropy generation. Air is used in the simulations. In addition, the maximum jet and swirling velocities considered in the present study results in laminar flow in the solution domain.

Fig. 2 shows the velocity vectors in the solution domain. When no swirling is introduced, a circulation cell next to the impinging jet and above the wall is generated. The velocity profile number effects the size of the circulation cell, i.e. the cell size increases as the velocity profile number reduces. The orientation of the circulation cell changes slightly in such a way that it extends slightly towards the jet exit. In this case, a uniform like jet profile generates a considerable shear layer across the jet, which in turn results in a circulation cell at the jet exit. Moreover, this shear layer drags the flow in the outer region of the cell to circulate at a high velocity. The flow leaving the solid wall mixes with the high velocity circulating flow. Consequently, the velocity in the circulation cell increases, which in turn, results in expansion of the cell and the orientation of the cell changes. This is also evident from Fig. 3, in which radial velocity component (v_r) is shown. In the case of low swirl velocity, the size and orientation of the circulation cell do not change much for velocity profile of $n = 1$. This is due to the gas jet velocity profile, which is almost a triangle shape. In this case, the velocity gradient between the jet outer radius and the outer region of the circulation cell is small, which in turn reduces the magnitude of the shearing force across the jet and the circulation cell. When the velocity profile number decreases to $n = 1/200$ (a uniform like velocity profile) the velocity gradient across the jet and the circulation cell outer re-

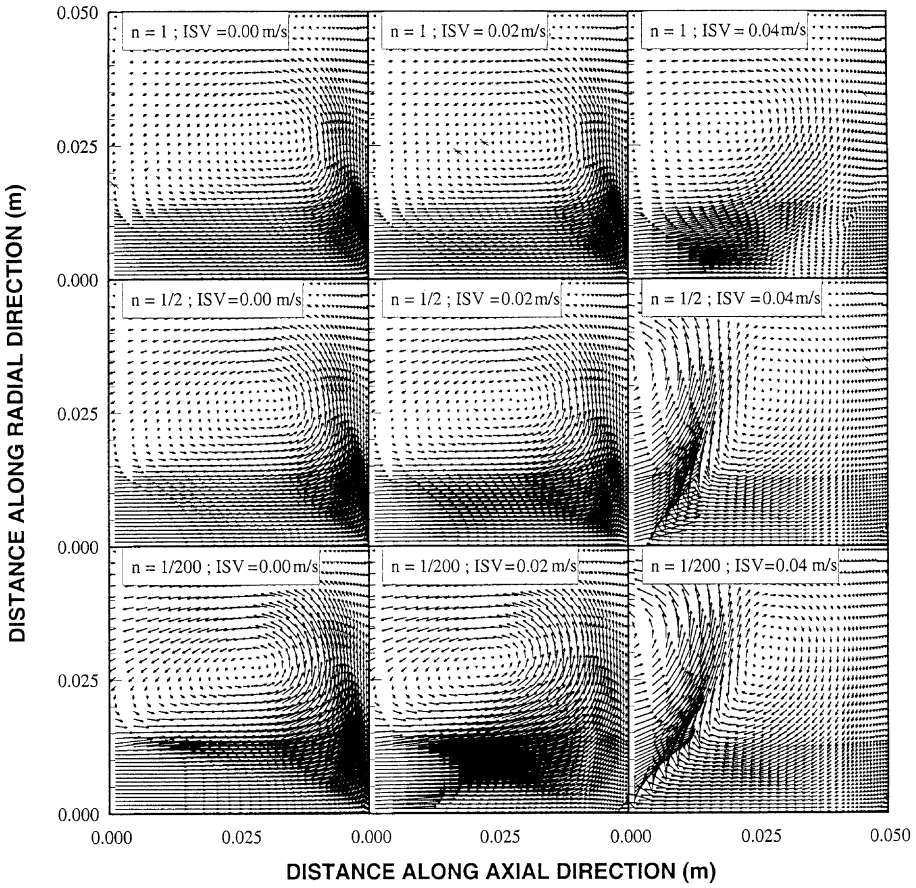

Fig. 2. Velocity vectors corresponding to different flow configurations. n is a velocity profile number and ISV represents inlet swril velocity.

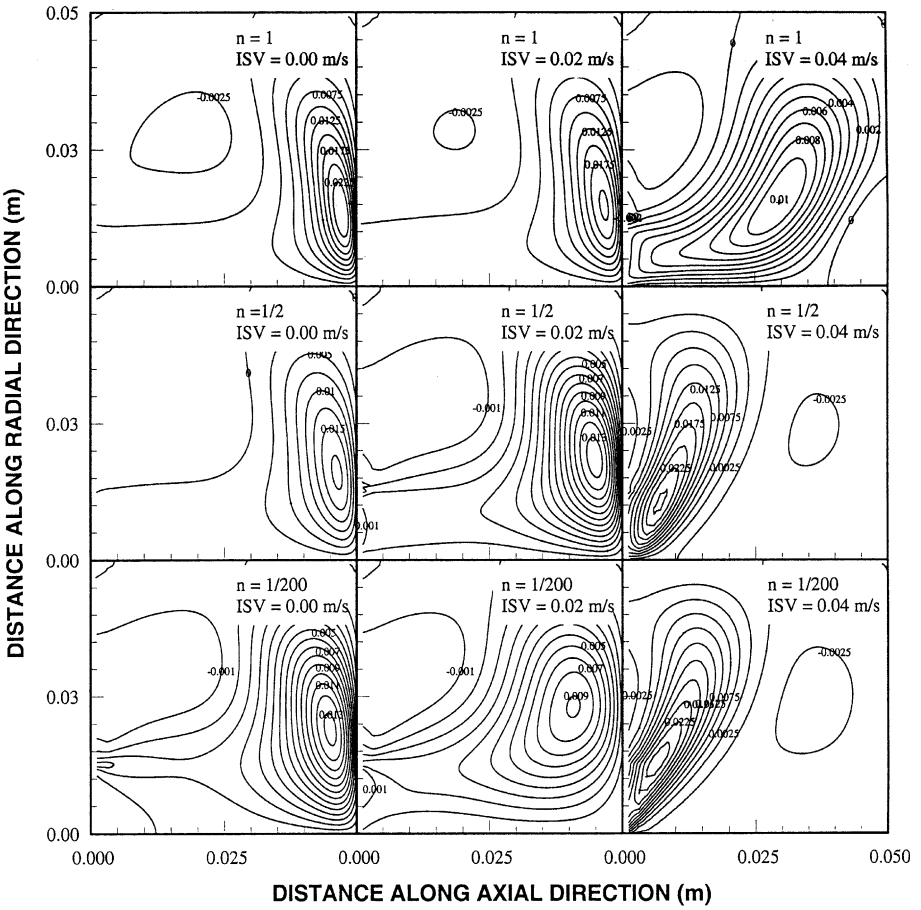

Fig. 3. Radial velocity (v_r) contours corresponding to different flow configurations. n is a velocity profile number and ISV represents inlet swril velocity.

gion become large. This in turn amplifies the shear force across the jet and the circulation cell. Consequently, the impinging jet influences the circulation cell, and the orientation as well as the size of the cell change. In the case of the high swirl velocity ($v = 0.04$ m/s), the flow field changes considerably. In the case of profile with $n = 1$, the circulation cell shifts away from the solid wall and moves towards the impinging jet. The inertia force in the radial direction becomes comparable to the inertia force in the axial direction. Moreover, a second circulation cell with clockwise rotation close to the stagnation region is generated. When the velocity profile number decreases to $n = 1/2$ while swirl velocity remains same ($v = 0.04$ m/s), the flow field changes and the size of the clockwise circulation cell increases. Therefore, the impinging jet spills towards the exit port rather than impinging onto a solid surface opposing the jet. In this case, the jet exiting velocity is parabolic and swirling of the jet results in the radial momentum component being larger than the axial momentum. Therefore, the jet exiting velocity spills and bends towards the radial direction. This can also be seen from Fig. 4, in which axial component of the velocity (v_z) is shown. As the velocity profile number further decreases to $n = 1/200$, the jet exiting profile becomes uniform like. The flow is similar to that corresponding to jet velocity profile number $n = 1/2$. However, jet exiting the nozzle expands further towards the exit port. This occurs because the radial momentum is considerably larger than the axial momentum. It should be noted that the uniform like velocity profile reduces the value of the maximum velocities in the axial direction, since the mass flow rate exiting the nozzle is same for all jet velocity profiles.

Fig. 5 shows the temperature contours in the control volume for different velocity profile number and swirling velocities. Temperature contours are highly concentrated in the region close to the nozzle exit and along the jet axis for low swirl velocities. In this case, radial momentum is negligibly small as compared to the axial momentum. Moreover, the effect of jet velocity profile

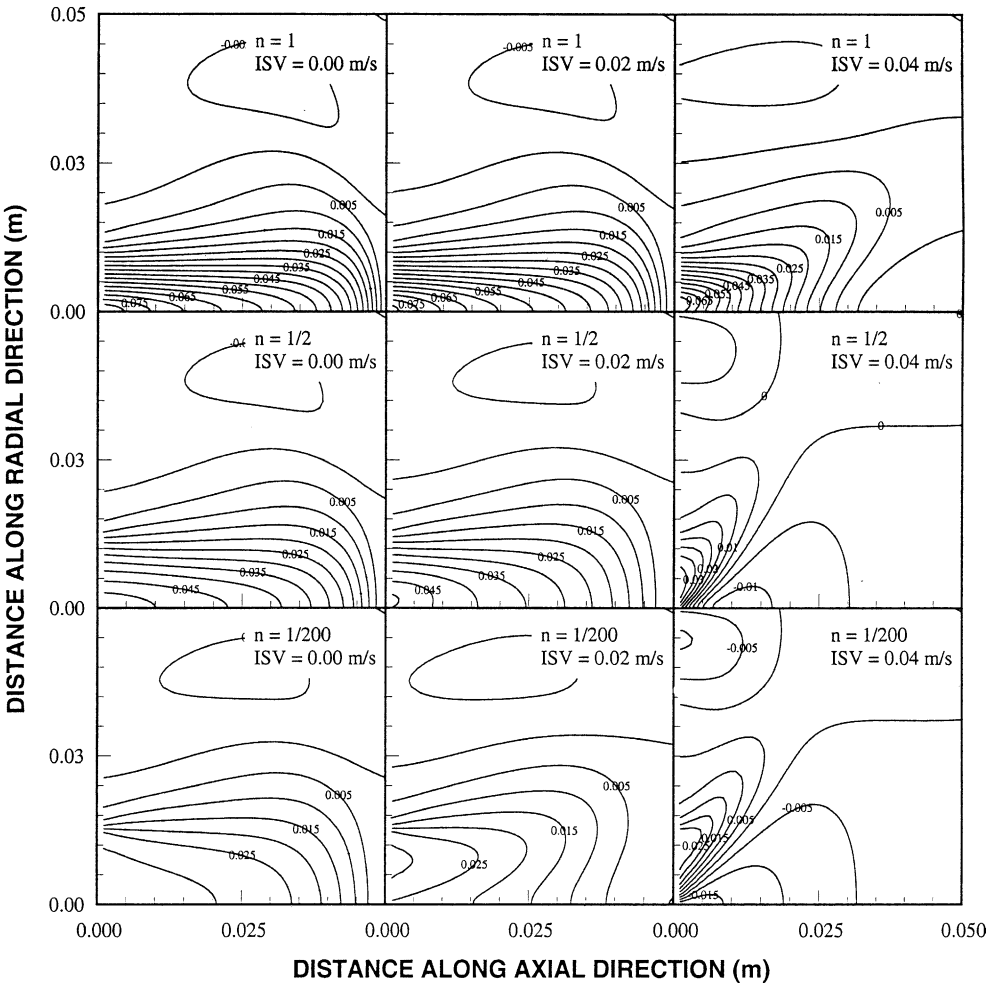

Fig. 4. Axial velocity (v_z) contours corresponding to different flow configurations. n is a velocity profile number and ISV represents inlet swril velocity.

number on the temperature contours is not significant when swirl velocity is zero. As the swirl velocity increases to 0.02 m/s, the flow field expands radially, which in turn extends the temperature contours away from the jet axis. This is more pronounced as the velocity number reduces to $n = 1/200$. The nozzle exit velocity is uniform like for the velocity profile number of $n = 1/200$, i.e. jet expands radially away from the jet axis since the maximum axial momentum reduces due to low maximum nozzle exit velocities. When the swirl velocity increases to 0.04 m/s, the radial momentum becomes almost as important as the axial momentum. This results in tilting the jet axis towards the radial direction and flow expands further in this direction. Since the temperature profiles follow the velocity profiles, temperature profiles also tilt similar to the velocity profiles.

Fig. 6 shows the volumetric entropy contours due to heat transfer for different jet profile numbers and swirl velocities. The entropy contours close to the nozzle exit are concentrated in the region close to the jet boundary. This is because of the temperature difference between the jet and its surroundings. In this case, a large temperature gradient occurs across the jet boundary. As the swirl velocity increases, the entropy contours extend further into the flow surrounding of the jet. However, the entropy contour is tilted towards the exit port, i.e. it bends in the radial direction. This is more pronounced as the jet velocity profile number reduces to $n = 1/200$. The low jet velocity profile number results in uniform like profile, which in turn, forces the flow to bend toward the radial direction. Consequently, temperature gradient across the jet and its surrounding becomes larger in the radial direction. This results in excessive entropy generation in the radial direction.

Fig. 7 shows the irreversibility ratio (I_p/I_{total}, ratio of irreversibility due to fluid friction over total irreversibility

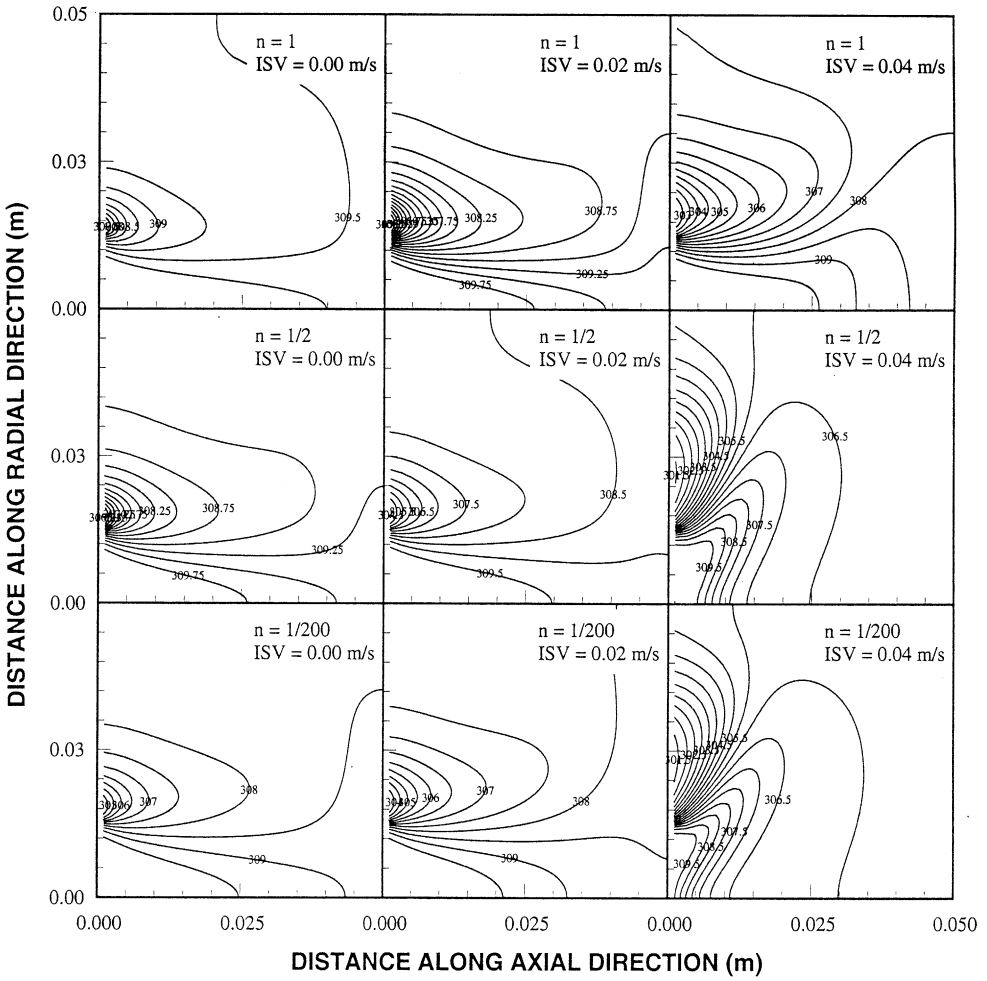

Fig. 5. Temperature contours corresponding to different flow configurations. n is a velocity profile number and ISV represents inlet swril velocity.

due to fluid friction and heat transfer) with velocity profile numbers for different swirl velocities. Increasing swirl velocity reduces the irreversibility ratio. This is more pronounced for the velocity profile numbers less than 1/5. Moreover, irreversibility ratio does not change considerably as velocity profile number increases (>1/5), provided that at high swirling velocity (ISV = 0.04 m/s) the irreversibility ratio remains the same for all velocity profile numbers. The high irreversibility ratio generation at low velocity profile numbers occurs because of the enhanced viscous dissipation across the jet and it's surrounding. In this case, the nozzle exit velocity profile number is uniform like and the velocity gradient across the jet and its boundary becomes high. This enhances the entropy generation and, therefore, irreversibility is enhanced. Increasing swirling velocity changes the orientation of the jet axis. This in turn improves the streamline curvaturing of the impinging jet in the region close to the solid wall and reduces the axial stress at the nozzle exit, i.e. the viscous dissipation decreases at the nozzle exit; consequently, the irreversibility contribution of viscous dissipation is small.

Fig. 8 shows the irreversibility ratio (I_t/I_{total}, the ratio of irreversibility due to heat transfer over the total irreversibility due to fluid friction and heat transfer) with velocity profile number and swirl velocity as variable. The behavior of the curves is opposite to those shown in Fig. 7. In this case, the irreversibility ratio increases as the velocity profile number increases to 1/5 and beyond 1/5, the irreversibility ratio remains almost constant with increasing velocity profile number. Moreover, the irreversibility ratio increases considerably as the swirl velocity increases. This indicates that the temperature gradient in the flow field especially across the jet outer boundary increases with swirl velocity, which, in turn, enhances the entropy generation. Consequently, uniform

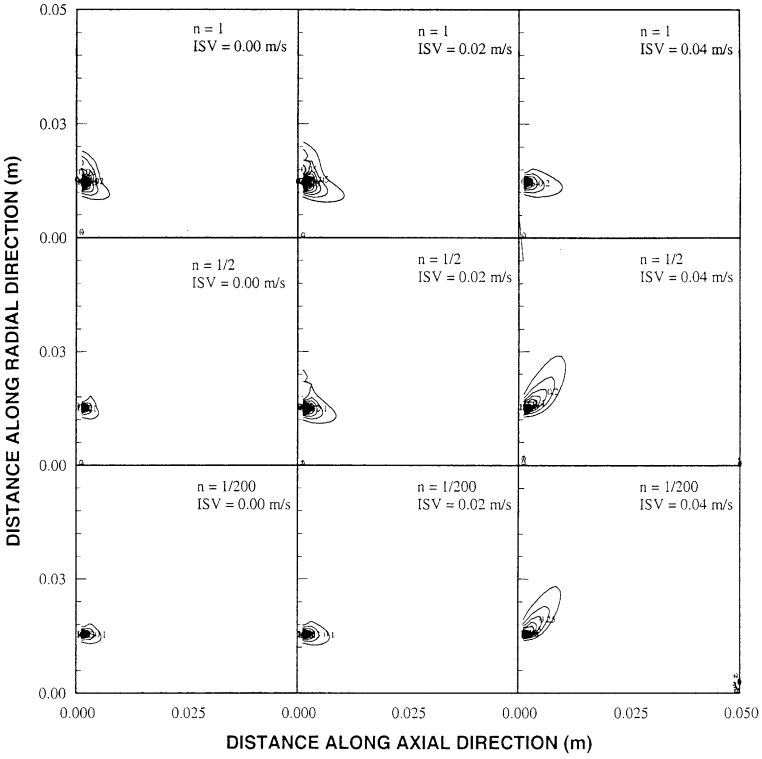

Fig. 6. Entropy contours due to heat transfer. n is a velocity profile number and ISV represents inlet swril velocity.

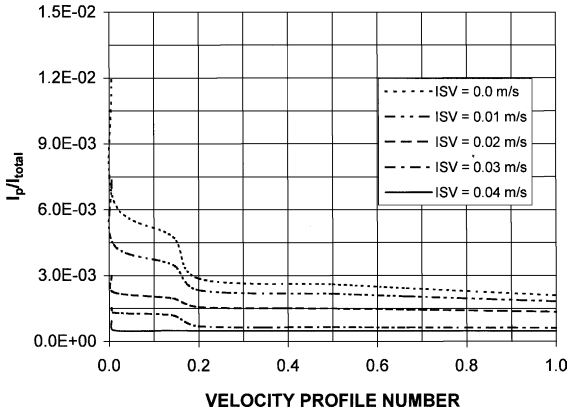

Fig. 7. Irreversibility ratio due to fluid friction with velocity profile number for different swirl velocities, ISV.

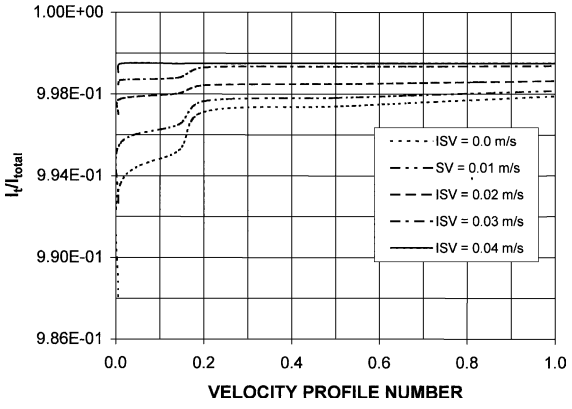

Fig. 8. Irreversibility ratio due to heat transfer with velocity profile number for different swirl velocities, ISV.

like heating in the flow field is suppressed by increasing swirling velocity. The irreversibility ratio due to heat transfer is considerably higher than that corresponding to fluid friction as shown in Fig. 7. This is because of the temperature difference between the jet and its surroundings, which results in large temperature gradient in the flow field.

5. Conclusions

Laminar confined and swirling jet impinging on a solid wall is considered. To examine the effects of jet velocity profile and swirl velocity on the flow field, a velocity profile number is introduced, while different swirl velocities are considered for each velocity profile

number in the simulations. To determine the amount of dissipation associated with the fluid friction and heat transfer, entropy analysis is carried out and irreversibility ratios are obtained for each flow configuration. In general, it is found that increasing swirling velocity tilts the axis of the impinging jet in the radial direction, in which case, irreversibility associated with the viscous dissipation reduces while its counter-part due to heat transfer increases. The effect of jet velocity profile number on the flow field and irreversibility is significant. The specific conclusions derived from the present study can be listed as follows:

1. The size and orientation of the circulation cell close to the solid wall change as the velocity profile number and swirl velocity change. A secondary circulation cell is generated close to solid wall as the swirl velocity increases. This is more pronounced as the velocity profile number reduces. In this case, radial momentum component becomes comparable to axial momentum, which in turn, results in tilting of the jet axis in the radial direction.
2. Temperature contours show similar behavior to the velocity profiles. Consequently, the effect of velocity profile number on the temperature contours is more pronounced when the swirl velocity increases. In this case, the temperature rise at the solid wall surface becomes insignificant, since the tilting of the jet axis prevents the hot flow to impinge normal to the wall surface.
3. Entropy generation across the jet outer boundary is considerably higher than any other location in the fluid. This occurs because of the rapid temperature change across the jet outer boundary, i.e. the temperature gradient is large in this region, which in turn results in high entropy generation rate.
4. The irreversibility associated with heat transfer is larger than that corresponding to fluid friction. The behavior of the irreversibility caused by fluid friction and heat transfer are almost opposite, i.e. increasing velocity profile number enhances the entropy generation due to heat transfer, but the entropy generation is suppressed with increasing velocity profile number. Moreover, the irreversibility due to heat transfer increases as swirl velocity increases while that corresponding to fluid friction decreases with increasing swirl velocity, i.e. swirl velocity has opposite effect on the irreversibility due to heat transfer and fluid friction.

Acknowledgements

The authors acknowledge the support of King Fahd University of Petroleum and Minerals. Dhahran, Saudi Arabia for this work.

References

[1] T.L. Yang, S.W. Chang, L.M. Su, C.C. Hwang, Heat transfer of confined impinging jet onto spherically concave surface with piston cooling application, JSME Int. J. B 42 (1999) 238–248.
[2] Y.H. Hung, L.S. Huang, Hydrodynamic characteristics for a round jet impingement with angular confinement, Int. J. Modell. Simul. 18 (1998) 180–189.
[3] H.J. Sheen, W.J. Chen, S.Y. Jeng, Recirculation zones of unconfined and confined annular swirling jets, AIAA J. 34 (1996) 572–579.
[4] V.N. Korovkin, Yu.A. Sokovishin, Variation of heat transfer in laminar wall jets with different initial velocity profiles, Appl. Therm. Sci. 2 (1989) 30–32.
[5] G.P. Romano, Investigation on time scales in a low Reynolds number jet flow using particle-tracking velocimetery, Appl. Sci. Res. 56 (1996) 209–220.
[6] I. Sezai, A.A. Mohamed, Three dimensional simulation of laminar rectangular impinging jets, flow structure and heat transfer, ASME J. Heat Transfer 121 (1999) 50–56.
[7] X.C. Lee, C.F. Ma, Q. Zheng, Y. Zhuang, Y.Q. Tian, Numerical study of recovery effect and impingement heat transfer with submerged circular jets of large Parndtl number liquid, Int. J. Heat Mass Transfer 40 (1997) 2647–2653.
[8] M.K. Drost, M.D. White, Numerical predictions of local entropy generation in an impinging jet, ASME J. Heat Transfer 113 (1991) 823–829.
[9] G. Ruocco, Entropy generation in conjugate heat transfer from a discretely heated plate to an impinging confined jet, Int. Comm. Heat Mass Transfer 24 (1997) 201–210.
[10] A. Bejan, Thermodynamics of an isothermal flow: the two-dimensional turbulent jet, Int. J. Heat Mass Transfer 34 (1991) 407–413.
[11] V. Arpaci, A. Selamet, Entropic efficiency of energy systems, Prog. Energy Combust. Sci. 18 (1992) 429–445.
[12] C.G. Carrington, Z.F. Sun, Second law analysis of combined heat and mass transfer in internal and external flows, Int. J. Heat Fluid Flow 13 (1992) 65–70.
[13] A. Bejan, A study of entropy generation in fundamental convective heat transfer, ASME J. Heat Transfer 101 (1979) 718–725.
[14] A. Bejan, Entropy Generation Minimization, CRC press, New York, 1995.
[15] S.V. Patankar, Numerical Heat Transfer and Fluid Flow, Hemisphere Publishing Company, Washington, DC, 1980.